Korean J. Chem. Eng., 35(1), 73-81 (2018)
DOI: 10.1007/s11814-017-0230-y

pISSN: 0256-1115
eISSN: 1975-7220

Cu/ZnO/AlOOH catalyst for methanol synthesis through CO_2 hydrogenation

EunGyoung Choi*,, KyoungHo Song*,**, SoRa An*,**, KwanYoung Lee**, MinHyeh Youn*, KiTae Park*, SoonKwan Jeong*, and HakJoo Kim*,†**

*Greenhouse Gas Research Laboratory, Korea Institute of Energy Research, Daejeon 34129, Korea
**Department of Chemical and Biological Engineering, Korea University, Seoul 02841, Korea
(*Received 18 April 2017 • accepted 15 August 2017*)

Abstract−Catalytic conversion of CO_2 to methanol is gaining attention as a promising route to using carbon dioxide as a new carbon feedstock. AlOOH supported copper-based methanol synthesis catalyst was investigated for direct hydrogenation of CO_2 to methanol. The bare AlOOH catalyst support was found to have increased adsorption capacity of CO_2 compared to conventional Al_2O_3 support by CO_2 temperature-programmed desorption (TPD) and FT-IR analysis. The catalytic activity measurement was carried out in a fixed bed reactor at 523 K, 30 atm and GHSV 6,000 hr^{-1} with the feed gas of CO_2/H_2 ratio of 1/3. The surface basicity of the AlOOH supported Cu-based catalysts increased linearly according to the amount of AlOOH. The optimum catalyst composition was found to be Cu : Zn : Al=40 : 30 : 30 at%. A decrease of methanol productivity was observed by further increasing the amount of AlOOH due to the limitation of hydrogenation rate on Cu sites. The AlOOH supported catalyst with optimum catalyst compositions was slightly more active than the conventional Al_2O_3 supported Cu-based catalyst.

Keywords: Methanol Synthesis, CO_2 Hydrogenation, FT-IR, Copper-based Methanol Synthesis Catalyst, Catalyst Support, CO_2 Adsorption, Temperature-programmed Desorption (TPD)

INTRODUCTION

Human activity since the Industrial Revolution has produced greenhouse gases (GHGs) such as carbon dioxide, methane and nitrous oxides, increasing the atmospheric carbon dioxide concentration from 280 ppm in 1,750 to 400 ppm in 2016 responsible for global warming and climate change [1,2]. Approximately 26 Gt of carbon dioxide is emitted to the atmosphere worldwide every year, which is 76% of the total emission of GHGs. To mitigate the emission of carbon dioxide from industrial plants, carbon dioxide capture & storage (CCS) technology is under operation and development. The captured carbon dioxide is injected in subsurface saline aquifers, reservoirs and aging oil fields for enhanced oil recovery (EOR) as means of permanent storage [3]. Nevertheless, there are still debates on the stability and environmental impacts of the sequestrated carbon dioxide as well as the financial costs for injection maintenance. In the 1990s, Olah proposed the utilization and conversion of the captured carbon dioxide to valuable fuels and chemicals using renewable energy source [4]. The captured carbon dioxide is used as a carbon source to convert it back to useful chemical products, especially methanol. He advocated the methanol economy in which methanol and dimethyl ether would replace fossil fuels as means of energy storage, ground transportation fuel and raw material for synthetic hydrocarbons and their products.

Methanol can be produced from a wide variety of sources, including still-abundant fossil fuels (natural gas, coal, oil shale, tar sands, etc.) as well as agricultural products and municipal waste, wood and varied biomass. It can also be made from chemical recycling of carbon dioxide.

The current world production of methanol is over 100 million tons per year. Although the activity of copper-containing catalysts in methanol synthesis has been known since the 1920s [5-8], Zn-Cr catalysts were used for a long time, while Cu-containing catalysts only remained an object of laboratory research. In the 1960s, a technological breakthrough was made by ICI, which patented the process over a Cu-Zn-Cr catalyst [9] and later a Cu-Zn-Al catalyst and revealed co-precipitation as its production method [10]. This invention allowed one to reduce the synthesis temperature from 673 to 503 K and the synthesis pressure from 200 to 50-100 atm. Due to the lower temperature, the selectivity of the process was dramatically improved. Starting from this point, the Cu-Zn-containing methanol synthesis catalysts have been studied intensively. The catalysts that are exemplified in the patent [10] by ICI had the cationic composition Cu : Zn : Al=60 : 30 : 10 and 75 : 19 : 6. But the technological application of methanol synthesis has preceded the full understanding of the underlying chemistry. The exact reaction mechanisms and the interplay of the surface properties of the catalyst with the feed gases are debated to this day. Among the most important open questions are the nature of the preferred carbon source for methanol - CO [11] or CO_2 [12] - and the effect of the Cu-Zn synergy, considered as having either no unique role [13], that is, mere structural promotion, or being essential for the active site [14,15]. Part of these discussions arise because of the difficulty of obtaining data for the industrial $Cu/ZnO/Al_2O_3$ catalysts under realistic working conditions [15]. Recent progress has shown that stepped and ZnOx-decorated Cu surfaces are crucial for the performance of industrial catalysts [16]. Furthermore, industrial catalysts contain low amounts of a refractory oxide as

†To whom correspondence should be addressed.
E-mail: hakjukim@kier.re.kr

structural promoter, in most cases up to 10% γ-Al_2O_3. Omitting any of the constituting elements drastically reduces the performance of the system.

Various efforts were also made to improve the activity and selectivity of the Cu-based catalysts for the direct hydrogenation of CO_2 to methanol. Since CO_2 is known as a weak acid gas, basic supports such as MgO, ZrO_2, TiO_2 were introduced instead of neutral or weak acidic Al_2O_3 support [17]. Alkali metal promoters were added in the same manner [18]. Addition of small amount of transition metal proved to increase the selectivity of C_2-C_3 higher alcohols [19].

In this work, we tried to develop a novel Cu-based catalyst for the direct hydrogenation of CO_2 to methanol. The surface and catalytic properties of the developed catalyst were fundamentally investigated considering the enhancement of its catalytic activity aroused from the basic AlOOH matrix. The bare AlOOH catalyst support was found to have increased adsorption capacity of CO_2 compared to the conventional Al_2O_3 support by CO_2 temperature-programmed desorption (TPD) and FT-IR analysis. The catalytic activity measurement was carried out in a fixed bed reactor at 523 K, 30 atm and GHSV 6,000 hr^{-1} with the feed gas of CO_2/H_2 ratio of 1/3. The surface basicity of the AlOOH supported Cu-based catalysts increased linearly according to the amount of AlOOH. The basicity of the AlOOH supported catalysts was generated solely from the basicity of the support AlOOH itself. Coordinatively unsaturated O^{2-} sites were generated at the edge of the crystal AlOOH structure. The optimum catalyst composition was found to be Cu : Zn : Al=40 : 30 : 30 at%. The adsorbed CO_2 at the edge of the crystal AlOOH was further hydrogenated by the spillover of the dissociatively adsorbed hydrogen on the neighbored active Cu sites. The decrease of methanol productivity was observed by further increasing the amount of AlOOH due to the limitation of hydrogenation rate on the relatively diminished Cu sites. The AlOOH supported catalyst with optimum catalyst compositions was slightly more active than the conventional Al_2O_3 supported Cu-based catalyst.

EXPERIMENTAL

The catalysts were prepared by the conventional co-precipitation method. 100 ml of deionized water was poured into a five-neck 500 ml flask and the temperature was adjusted to 353 K. The Cu/Zn/Al_2O_3 (Cu : Zn : Al=60 : 30 : 10 atomic%) catalyst was prepared similar to commercial catalysts. Cu, Zn, Al nitrates (Sigma Aldrich) were dissolved in deionized water so that the total concentration of the metal precursors was 1 M. The precursor solution was added in to the five-neck flask dropwise at a rate of 5 ml/min under stirring. The pH of the water was adjusted to 7-7.5 using a 1 M solution of sodium carbonate (Sigma Aldrich). The precipitates were aged at 353 K for 2 hr and were washed sufficiently with hot deionized water. The washed precipitates were dried at 383 K overnight, and subsequently calcined at 623 K for 2 hr under ambient atmosphere. Thus, prepared catalyst was denoted as [CZ-Al_2O_3 (6/3/1)]. [CZ-AlOOH (6/3/1)] catalyst was prepared under the same procedure, except that γ-AlOOH powder (Wenzhou Jingcheng Chemical) was suspended in the deionized water prior to the precipitation. Catalysts with different amount of AlOOH were prepared by proportionally varying the amount of Cu while the content of Zn was fixed at 30 atomic%. The catalysts were denoted as [CZ-AlOOH (5/3/2)], [CZ-AlOOH (4/3/3)] and [CZ-AlOOH (3/3/4)] indicating its cationic compositions in parenthesis. The preformed γ-Al_2O_3 was obtained by calcining γ-AlOOH powder at 623 K for 4 hr under ambient atmosphere. The pre-formed γ-Al_2O_3 supported catalyst was prepared under the same procedure except that γ-Al_2O_3 powder was used instead. The preformed γ-Al_2O_3 supported catalyst was denoted as [CZ-γ-Al_2O_3 (6/3/1)].

The reaction was carried in a fixed bed reactor with ⅜ inch of diameter. Precise flow control of reactants, carbon dioxide and hydrogen was attained with the aid of mass flow controller (5850E, Brooks) under pressurized reaction condition controlled by a back pressure regulator (26 Series, Tescom). Prior to reaction, the catalyst (1.2 g) was reduced in pure H_2 at a flow rate of 120 ml/min under atmospheric pressure. The reduction temperature was programmed to be increased from room temperature to 523 K and maintained for 1 hr. Then, the reactor was cooled to room temperature. The feed flow rate was adjusted to 160 ml/min with CO_2/H_2 ratio of 1/3 at a gas hourly space velocity of 6,000 hr^{-1}. The activities of the catalysts for CO_2 hydrogenation were measured at 523 K and 30 atm. At the exit of the reactor, liquid products were collected from the liquid collector prior equipped with a heat exchanger working with a cold fluid circulating system. The volumetric flow rate of gas phase product and unreacted feed gas was measured by the wet gas meter (Model W-NK, Shinagawa). The gas was sampled and injected to a gas chromatograph (7890B GC, Agilent) equipped with TCD and FID. The products were separated with the Carboxen 1000 column (⅛ inch×15 feet). Collected liquid products were analyzed with the aid of another GC (6890A GC, Agilent) equipped with the Carbowax 20 M column (30 m×0.32 mm×0.25 μm). Conversion of carbon dioxide and selectivity toward methanol and carbon balance were calculated using the following equations:

$$CO_2 \text{ conversion (\%)} = \left(1 - \frac{CO_2 \text{ molar flow rate in the product stream}}{CO_2 \text{ molar flow rate in the feed stream}}\right) \times 100\%$$

$$CH_3OH \text{ selectivity (\%)} = \left(\frac{CH_3OH \text{ molar flow rate in the product stream}}{\text{reacted } CO_2 \text{ molar flow rate}}\right) \times 100\%$$

$$\text{Carbon balance (\%)} = \left(\frac{[CO_2 + CO + CH_3OH] \text{ molar flow rate in the product stream}}{CO_2 \text{ molar flow rate in the feed stream}}\right) \times 100\%$$

Carbon balance was maintained within (100±1) % during each reaction experiment.

The BET surface area, pore volume and pore diameter of the prepared catalysts were measured by the nitrogen adsorption isothermals at 77 K (ASAP 2020, Micromeritics Instrument). The samples were thermally pre-treated at 473 K under vacuum for 2 hr.

The metal content of the prepared catalysts was determined by wavelength dispersive X-ray fluorescence (XRF) spectrometry (Primus II, Rigaku).

The basicity of the prepared catalysts was measured from the CO_2 temperature programmed desorption (CO_2-TPD) method (BEL-CAT, BEL Japan). The fresh catalyst (100 mg) was reduced with pure H_2 from room temperature to 573 K at a heating rate of 5 K/min and further kept at 573 K for 1 hr. The samples were cooled to 323 K under H_2 flow, then the gas flow was switched to CO_2 for an additional hour. The desorption was carried out by heating the samples at a rate of 10 K/min from 323 K to 873 K.

The copper surface area of the prepared catalysts was measured by H_2 pulse chemisorption (ASAP 2020 Chemisorption, Micromeritics Instrument). Samples were pre-treated under vacuum at 473 K for 2 hr. 14 points measurements with H_2 pulse injection from 10 to 500 mmHg were made giving 20 sec as equilibrium interval.

FT-IR spectra were recorded in transmission mode on a FT-IR spectrometer (Thermo Nicolet iS50, ThermoFisher Scientific) supplied with a DTGS detector. The powder samples diluted with KBr powder (1/100 w/w) were pressed into thin pellets using a pressure of 200 bar (sample mass about 150 mg). The transmittance spectra were obtained by collecting 32 scans at 4 cm^{-1} resolution.

RESULTS AND DISCUSSION

We examined the feasibility of boehmite γ-AlOOH as a novel catalyst support for the Cu-based methanol synthesis from CO_2 direct hydrogenation. Boehmite γ-AlOOH exhibits a lamellar structure within an orthorhombic symmetry [20]. Each layer constitutes the (OAlOH–HOAlO) stacking sequence in the x- and z-direction. The octahedral aluminums are surrounded by four tetrahedral oxygens and two hydroxyl groups as shown in Fig. 1 [21]. The cohesion of the stacked layers in the y-direction is ensured by hydrogen bonds between hydroxyl groups belonging to two consecutive layers and forming a zig-zag chain along the z-direction. Upon controlled calcination under air flow up to 623 K, boehmite γ-AlOOH undergoes a topotactic transformation into γ-Al_2O_3. In aluminum oxides, aluminum can have different types of coordinations with oxygen [22]. In transition aluminas, γ-Al_2O_3, the Al^{3+} ions occupy both octahedral and tetrahedral holes in the close-packed O_2^- array, and thus also possess tetrahedral coordination (AlO_4) [23].

Euzen et al. investigated the localization of basic and acid Brønsted sites on the boehmite nanosized particles using IR spectroscopy and density functional theory (DFT) calculations [20]. They reported that the strongest Brønsted acid sites were located on the basal surface of the boehmite nanosized particles, while the basic centers were on the edge plane.

Those crystal structures of the prepared supports were confirmed by the XRD as shown in Fig. 2. The diffractograms were in good agreement with the γ-AlOOH phase (JCPDS no. 21-1307). The γ-AlOOH phase with the orthorhombic crystal system had lattice parameters of a=3.7 nm, b=12.227 nm and c=2.868 nm. The γ-Al_2O_3 sample was obtained by calcinating γ-AlOOH at 673 K for

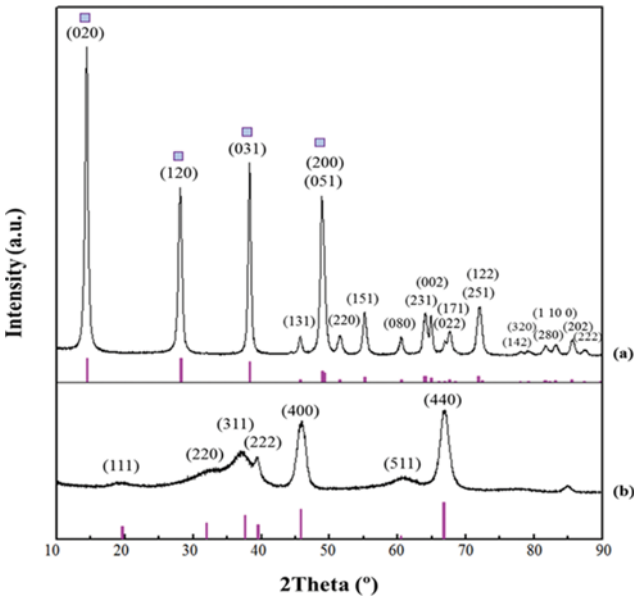

Fig. 2. XRD patterns of the prepared supports (a) γ-AlOOH, (b) γ-Al_2O_3.

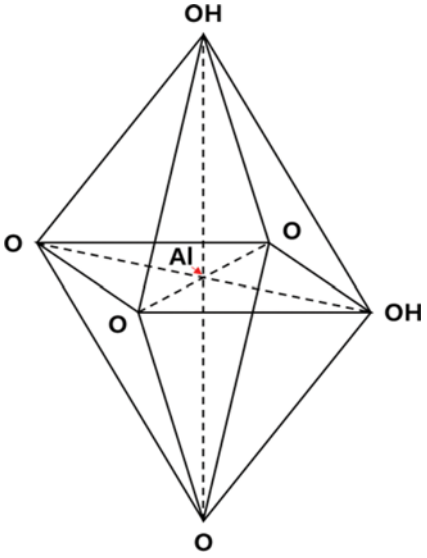

Fig. 1. The octahedral aluminums (AlO_6).

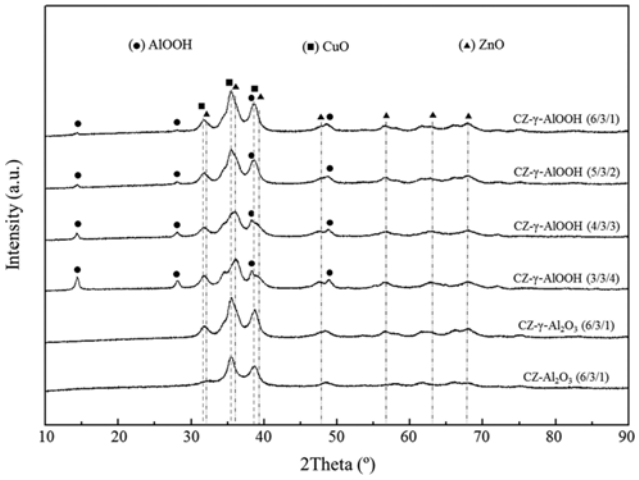

Fig. 3. XRD patterns of the prepared catalysts.

4 hr. The γ-Al_2O_3 phase had a cubic crystal system with cell parameters of a=7.924 nm, b=7.924 nm and c=7.924 nm (JCPDS no. 29-0063). Below the 623 K, γ-AlOOH tended to hold its structure, being able to be used as a catalyst support. The XRD patterns of prepared catalysts are shown in Fig. 3. By calcining at 623 K for 2 hr, metal carbonate precursors were clearly decomposed to their corresponding metal oxides. Diffraction patterns belonging to the CuO and ZnO phases were detected in all catalysts. The main peak of γ-AlOOH was clearly identified in the CZ-γ-AlOOH catalysts with the increasing intensity proportionally to its content.

For the analysis of surface functional groups and the chemical bonding with CO_2, γ-AlOOH and γ-Al_2O_3 were characterized by FT-IR spectroscopy, as illustrated in Fig. 4. The observed vibrational transitions and assignments of the supports are summarized in Table 1 [22,24,25]. For γ-AlOOH, as the OH directions form zig-zag chains between the planes of oxygen ions, two distinct OH stretching modes were observed at 3,101 cm^{-1} and 3,281 cm^{-1} [22, 24,25]. These bands can be assigned as ν_s(Al)O-H and ν_{as}(Al)O-H stretching vibrations. An intense band at 1,073 cm^{-1} and a shoulder at 1,150 cm^{-1} were observed, which were assigned to the symmetric and asymmetric bending modes of the (Al)O-H groups respectively [22,24,25]. Very broad bands at 765, 637 and 568 cm^{-1}

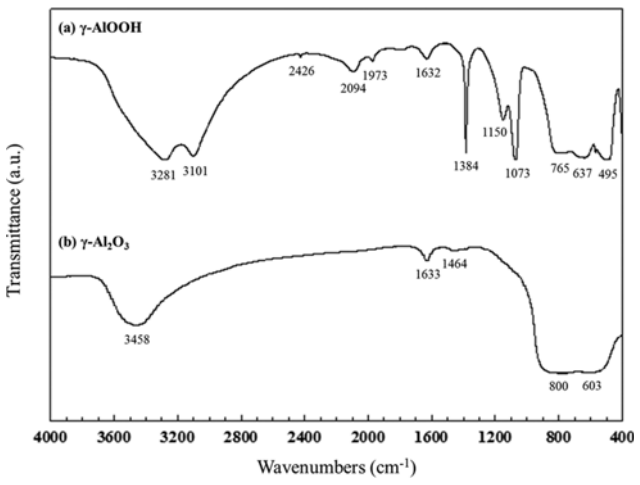

Fig. 4. FT-IR spectra of γ-AlOOH and γ-Al_2O_3 supports.

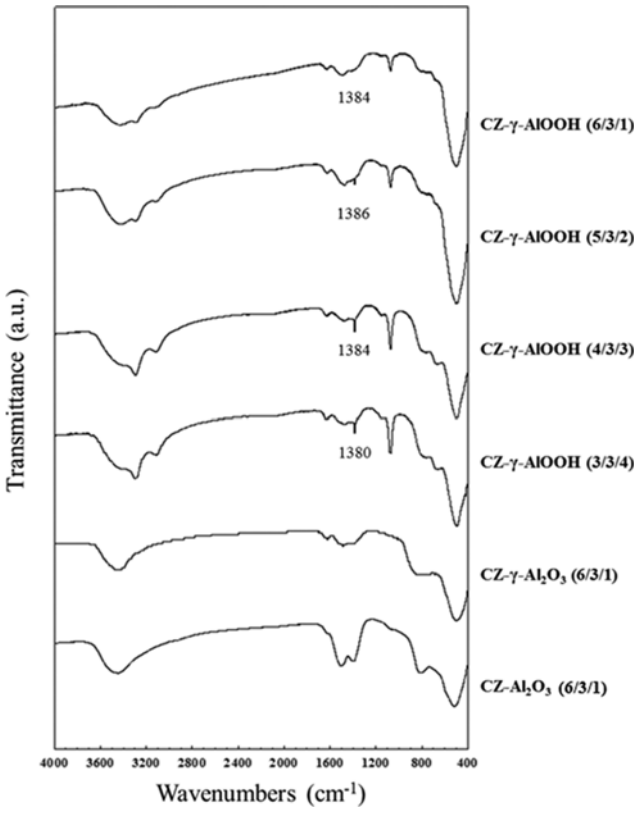

Fig. 5. FT-IR spectra of the prepared catalysts.

Table 1. Observed vibrational transitions (cm^{-1}) and assignments of the supports

γ-AlOOH	γ-Al_2O_3	Assignment
~3450	3458	Stretching of adsorbed water
3281		ν_{as} (Al)O-H
3101		ν_s (Al)O-H
2426		ν_{as} end on Al-CO_2 complexs
2094		Vibrational overtones of AlOOH surface -OH groups
1973		
1632	1633	Bending of absorbed water
	1464	Bicarbonate
1384		Unidentate (Monodentate) carbonate
1150		δ_{as} Al-O-H
1073		δ_s Al-O-H
765		
637	800	ν AlO_6
568		
495		δ AlO_6
	603	ν AlO_4

ν_{as}: asymmetric stretching, ν_s: symmetric stretching, δ_{as}: asymmetric bending, δ_s: symmetric bending

were assigned to the stretching modes of octahedral coordination of (AlO_6), while the band at 495 cm^{-1} to the bending mode of (AlO_6) [22,26,27]. For γ-Al_2O_3, very broad bands were observed for stretching vibration of Al-O in the tetrahedral (AlO_4) and octahedral (AlO_6) coordination at 800 cm^{-1} and in the region of 500-750 cm^{-1}, respectively [22]. Wide bands at 3,450 and 1,640 cm^{-1} were assigned to the stretching band of water molecules from moisture contained in air atmosphere [22]. Since γ-AlOOH and γ-Al_2O_3 were exposed in air atmosphere during KBr pellet sample preparation, CO_2 present in air was adsorbed on the basic sites of both catalyst supports. For γ-AlOOH, CO_2 was adsorbed as unidentate carbonate at 1,384 cm^{-1}, while for γ-Al_2O_3 as bicarbonate at 1464 cm^{-1}. The adsorbed phases of CO_2 on the prepared Cu based catalysts were also confirmed by FT-IR spectra as shown in Fig. 5. The adsorbed band of the unidentate carbonate was intensified proportionally according to the content of γ-AlOOH. In the CZ-γ-Al_2O_3 catalyst, the content of γ-Al_2O_3 was too small to confirm bicarbonate adsorption band.

Apesteguia et al. reported that CO_2 was adsorbed on high, medium and low strength basic sites as unidentate carbonate, bidentate carbonate and bicarbonate species respectively as illustrated in Scheme 1 based on precedent work of Morterra et al. and Fujimoto et al. [28-30]. So, γ-AlOOH was found to strongly adsorb CO_2 on the high strength basic site and can be used as a chemical promoting support for development of catalysts using CO_2 as reactant.

For quantitative and qualitative analysis of basic sites present on γ-AlOOH and γ-Al_2O_3, CO_2-TPD analysis was performed and the results presented in Fig. 6. Fig. 7 Shows the CO_2 desorption profiles obtained for the prepared catalysts. All profiles can be deconvoluted into three Gaussian peaks. The number of basic sites was calculated and summarized in Table 2 from the deconvolution of the CO_2-TPD profiles by assuming three basic sites of different strength. Site a was assigned to the low strength basic site, while sites b and g as medium and high strength basic site, respectively, as mentioned above. For γ-AlOOH support, strong basic sites were noticeably produced with considerable number of moderate basic sites. However, for γ-Al_2O_3 support, the number of total basic

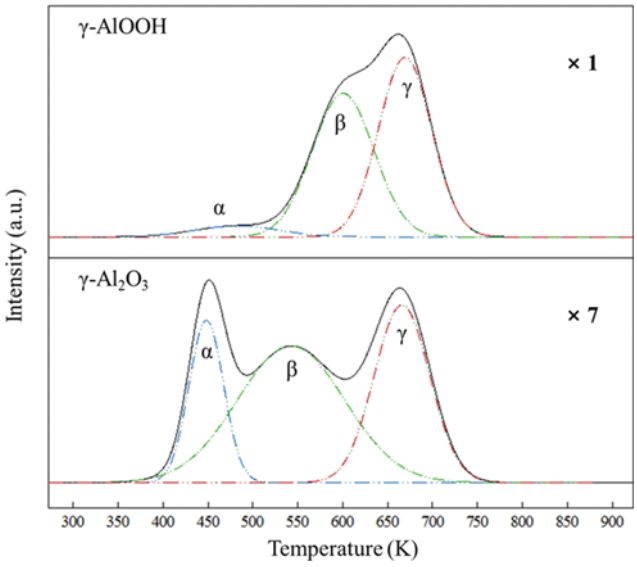

Fig. 6. CO_2-TPD profiles of γ-AlOOH and γ-Al_2O_3 supports.

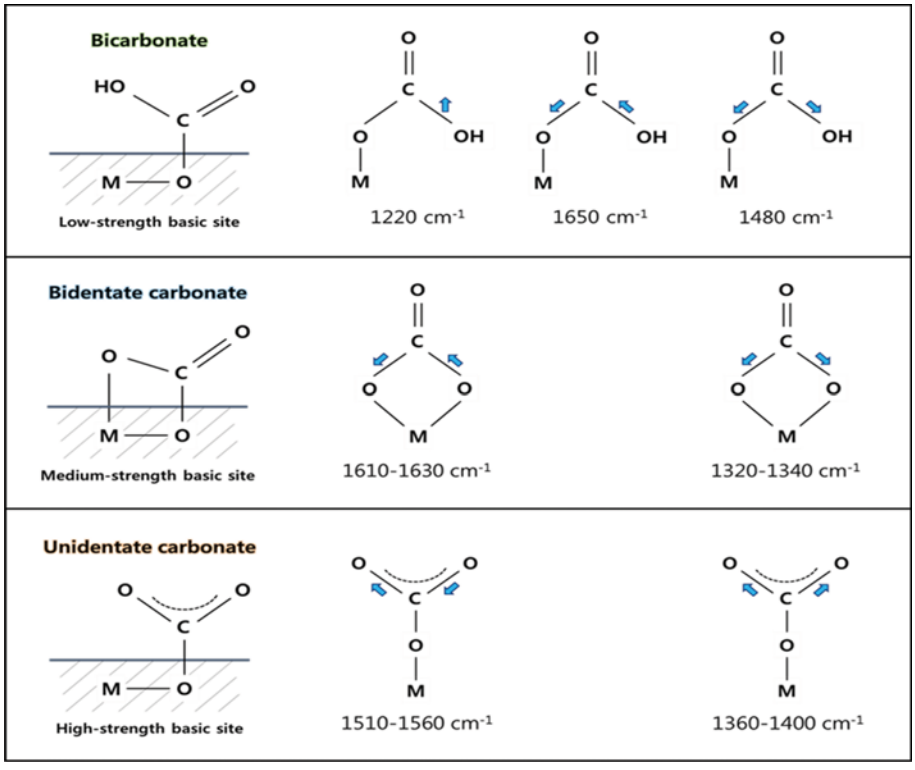

Scheme 1. IR bands of adsorbed CO_2 surface species.

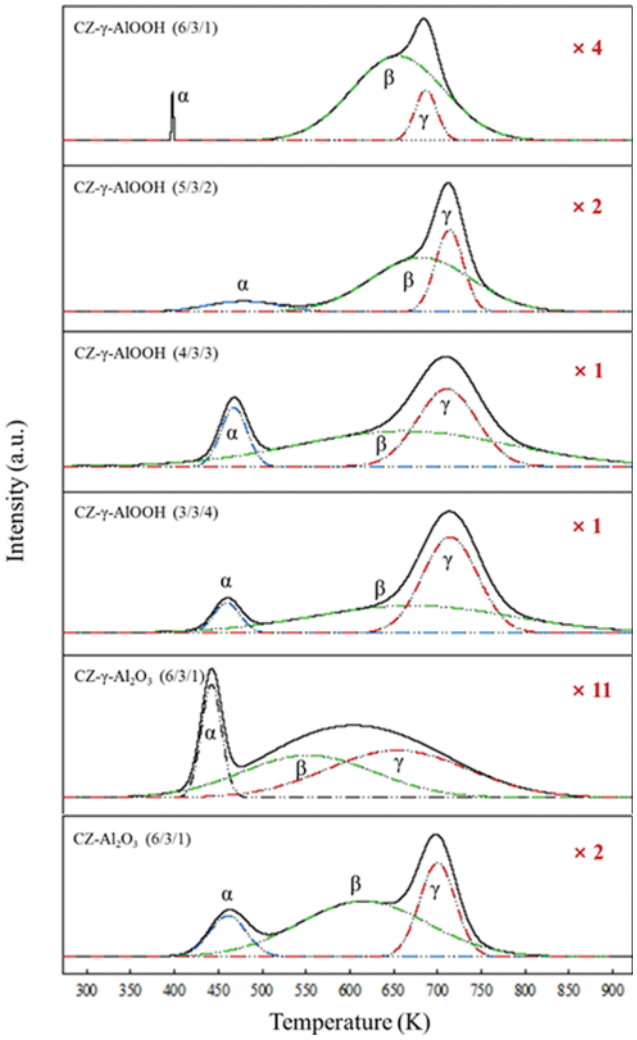

Fig. 7. CO_2-TPD profiles of the prepared catalysts.

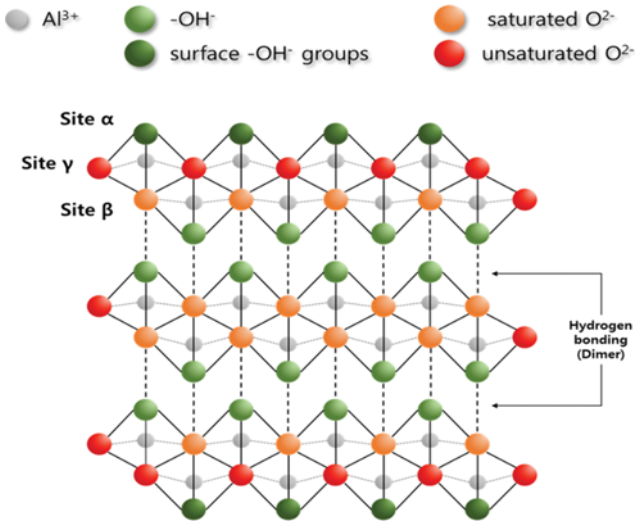

Fig. 8. Basic sites (α, β, γ) in the γ-AlOOH structure.

sites was remarkably reduced. The role of Al_2O_3 support in the conventional Cu/ZnO/Al_2O_3 methanol synthesis catalyst was reported in the literature and generally believed to be the physical promoter providing high specific surface area for the bulk catalyst, and preventing the sintering of active species copper for enhancing its catalytic stability. From the high CO_2 adsorptivity, γ-AlOOH can be considered as a novel support for Cu-based methanol synthesis catalyst from direct CO_2 hydrogenation. From the results of CO_2-TPD analysis of the prepared catalysts as presented in Fig. 7 and Table 2, number of total basic sites as well as that of the strong basic site γ increased with the content of γ-AlOOH. This phenomenon can be explained by the fact that the majority of the basic sites present on the prepared catalyst stemmed from the added γ-AlOOH itself.

In γ-AlOOH structure (Fig. 8) [31], the weakly basic sites were ascribed to surface hydroxyl groups, the moderately basic sites were related to saturated metal-oxygen pairs, and the strongly basic sites were associated with coordinatively unsaturated O^{2-} ions present at the edge of the crystal structure. Three species of adsorbed CO_2, bicarbonate species, bidentate carbonates, and unidentate carbonates, were formed on these three types of surface basic sites, respectively. The adsorption and dissociation of hydrogen occur over the Cu site, and three species of adsorbed CO_2 are formed on the surface weakly, moderately and strongly basic sites (basic sites α, β and γ), respectively. The adsorption of bicarbonate species on the basic sites α is weak and easy to desorb to form CO_2 again.

According to the literature, the optimum cationic composition

Table 2. Number of basic sites present in the prepared catalysts

Catalyst	Number of total basic sites (μmol/g)	Number of basic sites with different strength (μmol/g)		
		Site α	Site β	Site γ
γ-AlOOH	41.7	2	19.4	20.3
γ-Al_2O_3	6.5	2.2	1.3	3.1
CZ-γ-AlOOH (6/3/1)	3.8	0.1	3	0.8
CZ-γ-AlOOH (5/3/2)	6.6	0.6	4.3	1.8
CZ-γ-AlOOH (4/3/3)	10.4	2.8	3	4.6
CZ-γ-AlOOH (3/3/4)	14.8	2.3	4.4	8.1
CZ-γ-Al_2O_3 (6/3/1)	1.3	0.4	0.3	0.6
CZ-Al_2O_3 (6/3/1)	8.8	1.1	5.2	2.5

Table 3. Physicochemical properties of the prepared catalysts and supports

Catalyst	Chemical composition (atomic%)[a]			SA_{BET} (m^2/g)	Pore volume (cm^3/g)	Pore size (Å)	Cu surface area (m^2/g)
	Cu	Zn	Al				
γ-AlOOH	-	-	-	120.5	0.6	202.6	-
γ-Al_2O_3	-	-	-	147.4	0.7	199.8	-
CZ-γ-AlOOH (6/3/1)	63.3	28.8	7.9	88.2	0.4	188.9	10.8
CZ-γ-AlOOH (5/3/2)	52.9	28.5	18.7	92.2	0.5	216.7	10.9
CZ-γ-AlOOH (4/3/3)	42.6	29.4	27.9	96.9	0.6	229.4	10.5
CZ-γ-AlOOH (3/3/4)	34.1	30.9	35.0	104.3	0.6	248.9	7.2
CZ-γ-Al_2O_3 (6/3/1)	66.4	30.6	3.0	97.5	0.5	186.2	6.1
CZ-Al_2O_3 (6/3/1)	61.7	28.3	10.1	99.9	0.4	177.0	15.9

[a]XRF data

of the conventional Cu/ZnO/Al_2O_3 methanol synthesis catalyst was Cu : Zn : Al=60 : 30 : 10 (atomic%) based on the registered patent of ICI [10]. For proper comparison, CZ-γ-AlOOH catalyst having the same cationic composition was prepared and investigated. To enlarge the effect of γ-AlOOH addition, catalysts with different amount of Al were prepared by proportionally varying the amount of Cu while the content of Zn was fixed at 30 atomic%. The metal compositions of the prepared catalysts measured by XRF spectrometer are presented in Table 3. The compositions of the prepared catalysts were in close agreement with the nominal compositions.

The specific surface areas of the prepared supports and catalysts measured by BET instrument are summarized in Table 3. The γ-AlOOH had a moderate specific surface area of 120.5 m^2/g but lower than that of γ-Al_2O_3. In the CZ-γ-AlOOH catalyst, BET surface area tended to increase proportionally to the content of γ-AlOOH.

The catalyst activity measurement results at 523 K, 30 atm are given in Table 4. There was a linear relationship between the amount of total basic sites and the selectivity toward methanol as shown in Fig. 9. Fujitani et al. reported that CO_2 was mainly adsorbed on ZnO and further hydrogenated to methanol with the spillover of hydrogen adsorbed on Cu for the synthesis of methanol from carbon dioxide [14,32]. Considering that reaction mechanism introduction of basic sites enhancing the adsorption of the reactant CO_2 could increase the catalytic activity as well as the selectivity toward methanol. Recently, Sun et al. [30,33-35] suggested that the unidentate carbonate (site *γ*) was active to react

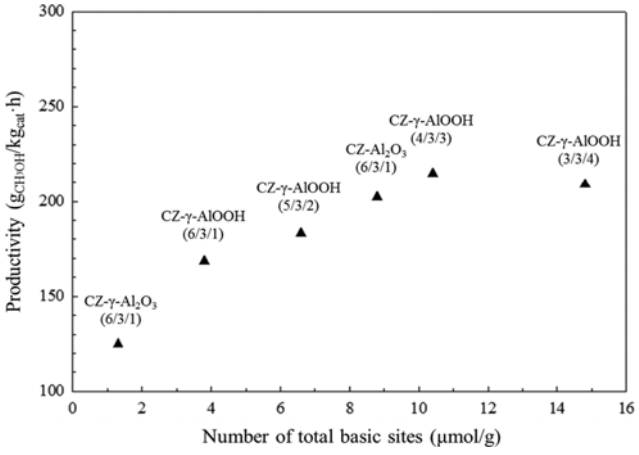

Fig. 9. Relationship between the amount of total basic sites and the selectivity toward methanol (Reaction conditions: T=523 K, P=30 atm, GHSV=6,000 hr^{-1}).

with the surface atomic hydrogen from the spillover of the dissociatively adsorbed hydrogen molecule on the metallic Cu, stepwise forming HCOO, H_2COO, H_2COOH, H_3COOH, and finally CH_3OH and H_2O. While the bidentate carbonate (site *β*) reacted with the hydrogen atom to produce CO and H_2O by reverse water-gas shift reaction (RWGSR). The proposed direct hydrogenation of CO_2 to methanol by the formate pathway requires strong basic *γ* site generated from the coordinatively unsaturated oxygen atoms present on the Zn-Al matrix. Le Valant et al. built a mathematical

Table 4. Catalytic activity of the prepared catalysts

Catalyst	Selectivity (C-mol%)		CH_3OH yield (%)	Productivity (g_{CH3OH}/kg_{cat}·h)
	CO	CH_3OH		
CZ-γ-AlOOH (6/3/1)	68.2	31.8	6.8	168.5
CZ-γ-AlOOH (5/3/2)	65.3	34.7	7.0	183.2
CZ-γ-AlOOH (4/3/3)	62.0	38.0	8.0	214.7
CZ-γ-AlOOH (3/3/4)	62.5	37.5	7.8	208.9
CZ-γ-Al_2O_3 (6/3/1)	71.6	28.4	4.7	125.0
CZ-Al_2O_3 (6/3/1)	62.5	37.5	7.7	202.5

Reaction conditions: T=523 K, P=30 atm, GHSV=6,000 hr^{-1}

Table 5. Catalytic activity at 50 atm of the prepared catalysts

Catalyst	Selectivity (C-mol%)		CH_3OH yield (%)	Productivity (g_{CH3OH}/kg_{cat}·h)
	CO	CH_3OH		
CZ-γ-AlOOH (4/3/3)	44.1	55.9	14.1	348.7
CZ-Al_2O_3 (6/3/1)	45.6	54.4	13.5	325.6

Reaction conditions: T=523 K, P=50 atm, GHSV=6,000 hr^{-1}

model based on the assumption that the creation of active sites, and therefore the synergy, was directly linked to the contacts between Cu and ZnO during the reduction of the catalyst [36,37]. The quantitative information generated by the model was the concentration of contacts, which described the ability of metal ions to migrate according to the Kirkendall effect. The evolution of concentration of contacts versus Zn content matched the catalyst activity evolution, which shows that the migration could be controlled and improved by favoring contacts between the two metals during the synthesis. For the CZ-γ-Al_2O_3 catalyst prepared by ICI's recipe, 2.5 μmol/g of strong basic site γ was generated even though bare γ-Al_2O_3 had poor basicity. Considering the work of Sun et al. and Le Valant et al., this fact can be explained by the surface reconstruction of Zn-Al matrix generating defect sites with coordinatively unsaturated oxygen atoms during the catalyst preparation and activation process. This phenomenon can be clarified by the fact that the preformed γ-Al_2O_3 supported catalyst CZ-Al_2O_3 (6/3/1) had only 0.6 μmol/g of strong basic site γ. Since Al was introduced as γ-Al_2O_3 powder with fully developed crystal structure, surface reconstruction of Zn-Al matrix seems difficult to occur during the catalyst preparation process. The same explanation seems to be available for the CZ-γ-AlOOH catalyst, where Al was introduced as γ-AlOOH powder. On the other hand, since γ-AlOOH had 20.3 μmol/g of strong basic site γ, the strong basic site of the CZ-γ-AlOOH catalyst was thought to be generated from the property of the bare γ-AlOOH support. To the best of our knowledge, the optimum cationic composition of the CZ-γ-AlOOH catalyst is Cu : Zn : Al=40 : 30 : 30 (atomic%). When the Al content was further increased up to 30 atomic%, the amount of strong basic site γ was enlarged proportionally to the introduced amount of γ-AlOOH. But methanol selectivity started to decrease. As mentioned, formate intermediate reaction mechanism favors the reaction of adsorbed CO_2 with atomic hydrogen from the spillover of the dissociatively adsorbed hydrogen molecule on the metallic Cu. From Table 3, Cu surface area of CZ-γ-AlOOH (3/3/4) started to decrease to 7.2 m^2/g, more than 34% loss compared with those of CZ-γ-AlOOH (6/3/1), (5/3/2), (4/3/3) catalysts. Since the amount of metallic Cu was reduced with increased Al loading, hydrogenation of the adsorbed CO_2 species seemed to be limited by the diminution of the hydrogen spillover on the metallic Cu.

The hydrogenation reaction seemed difficult to proceed on this weak basic site α. The adsorbed CO_2 on both the β and γ basic sites underwent stepwise hydrogenation to HCOO, H_2COO, H_2COOH and H_2CO with atomic hydrogen (H) being supplied by means of H spillover from Cu. In addition, the C=O bond of H_2CO absorbed on strongly basic sites may be activated to react with surface atomic hydrogen to form methanol attributed to the strong C-γ bond (Fig. 8). However, the C=O bond of H_2CO adsorbed on moderately basic sites are relatively stable due to the weaker C-β interaction, which results in the H_2CO species preferring to dehydrogenate to form CO rather than be hydrogenated into methanol [35].

To confirm the pronounced AlOOH effect, an additional activity test was performed at the reaction pressure of 50 atm. The catalysts were compared with the CZ-Al_2O_3 catalyst as reference catalyst and the CZ-γ-AlOOH (4/3/3) catalyst, had the highest selectivity and yield at the reaction pressure of 30 atm. The catalytic activity measurement results at 523 K, 50 atm are summarized in Table 5. The conversion as well as the selectivity to methanol tended to increase with the reaction pressure among the tested catalysts. In particular, the activity of the CZ-γ-AlOOH (4/3/3) catalyst was excellent even at 50 atm.

CONCLUSIONS

The introduction of γ-AlOOH as Al precursor was found to be effective in the preparation of Cu based catalysts with strong basic sites available for stepwise hydrogenation of CO_2 to methanol via formate pathway. The bare AlOOH catalyst support had increased adsorption capacity of CO_2 compared to the conventional Al_2O_3 support by CO_2 temperature-programmed desorption (TPD) and FT-IR analysis. The basicity of the AlOOH supported catalysts was generated solely from the basicity of the support AlOOH itself, increasing with the amount of loaded AlOOH. Coordinatively unsaturated O^{2-} sites generated at the edge of the crystal AlOOH structure were assigned as the origin of the surface basicity. The optimum cationic composition of CZ-γ-AlOOH catalyst was found to be Cu : Zn : Al=40 : 30 : 30 (atomic%). The decrease of methanol productivity was observed by further increasing the amount of AlOOH due to the limitation of hydrogenation rate on the relatively diminished Cu sites. The AlOOH supported catalyst with optimum catalyst compositions was slightly more active than the conventional Al_2O_3 supported Cu-based catalyst.

ACKNOWLEDGEMENTS

This work was financially supported by the Grant-in-aid from the Ministry of Science, ICT and Future Planning and Korea Institute of Energy Research (Project B7-2431 - Development of CO_2 capture, conversion and utilization technologies).

REFERENCES

1. D. L. Hartmann, *Global Physical Climatology (2nd Ed.)* (2016).

2. D. Bratt, *Catalytic CO_2 Hydrogenation - Literature Review: Technology Development Since 2014* (2016).
3. *Storing CO_2 through Enhanced Oil Recovery - Combining EOR with CO_2 storage (EOR+) for profit*, OECD/IEA (2015).
4. G. A. Olah, G. K. S. Prakash and A. Goeppert, *J. Am. Chem. Soc.*, **133**, 12881 (2011).
5. M. Patart, France Patent, FR540343 (1921).
6. E. Audibert, *Fuel Sci. Pract.*, **5**, 170 (1926).
7. P. K. Frolich, M. R. Fenske, P. S. Taylor and C. A. Southwick, *Ind. Eng. Chem.*, **20**, 1327 (1928).
8. D. Cornthwaite, US Patent, 3,923,694 (1974).
9. P. Davies and F. F. Snowdon, US Patent 3,326,956 (1967).
10. J. T. Gallagher and J. M. Kidd, Patent GB1159035 (1969).
11. K. Klier, V. Chatikavanij, R. G. Herman and G. W. Simmons, *J. Catal.*, **74**, 343 (1981).
12. G. C. Chinchen, P. J. Denny, D. G. Parker, M. S. Spencer and D. A. Whan, *Appl. Catal.*, **30**, 333 (1987).
13. K. C. Waugh, *Catal. Lett.*, **142**, 1153 (2012).
14. J. Nakamura, Y. Choi and T. Fujitani, *Top. Catal.*, **22**, 277 (2003).
15. M. Behrens, F. Studt, I. Kasatkin, S. Kühl, M. Hävecker, F. Abild-Pedersen, S. Zander, F. Girgsdies, P. Kurr, B.-L. Kniep, M. Tovar, R. W. Fischer, J. K. Nørskov and R. Schlögl, *Science*, **336**, 893 (2012).
16. F. Studt, M. Behrens, E. L. Kunkes, N. Thomas, S. Zander, A. Tarasov, J. Schumann, E. Frei, J. B. Varley, F. Abild-Pedersen, J. K. Nørskov and Robert Schlögl, *Chem. Cat. Chem.*, **7**, 1105 (2015).
17. G. Bonura, M. Cordaro, C. Cannilla, F. Arena and F. Frusteri, *Appl. Catal. B Enviorn.*, **152-153**, 152 (2014).
18. D. Li, N. Ichikuni, S. Shimazu and T. Uematsu, *Appl. Catal. A Gen.*, **172**, 351 (1998).
19. E. Heracleous, E. T. Liakakou, A. A. Lappas and A. A. Lemonidou, *Appl. Catal. A Gen.*, **455**, 145 (2013).
20. P. Raybaud, M. Digne, R. Iftimie, W. Wellens, P. Euzen and H. Toulhoat, *J. Catal.*, **201**, 236 (2001).
21. L. Farkas, P. Gad and P. E. Werner, *Mater. Res. Bull.*, **12**, 1213 (1977).
22. G. K. Priya, P. Padmaja, K. G. K. Warrier, A. D. Damodaran and G. Aruldhas, *J. Mater. Sci. Lett.*, **16**, 1584 (1997).
23. C. Morterra, C. Emanuel, G. Cerrato and G. Magnacca, *J. Chem. Soc. - Faraday Trans.*, **88**, 339 (1992).
24. K. A. Wickersheim and G. K. Korpi, *J. Chem. Phys.*, **42**, 579 (1965).
25. J. J. Fripiat, H. J. Bosmans and P. G. Rouxhet, *J. Phys. Chem.*, **71**, 1097 (1967).
26. D. Mazza, M. Vallino and G. Busca, *J. Amer. Ceram. Soc.*, **75**, 1929 (1992).
27. P. McMillan and B. Piriou, *J. Non. Cryst. Solids*, **53**, 279 (1982).
28. C. Morterra, G. Ghiotti, F. Boccuzzi and S. Coluccia, *J. Catal.*, **51**, 299 (1978).
29. R. Philipp and K. Fujimoto, *J. Phys. Chem.*, **96**, 9035 (1992).
30. J. I. Di Cosimo, V. K. Díez, M. Xu, E. Iglesia and C. R. Apesteguía, *J. Catal.*, **178**, 499 (1998).
31. V. P. Pakharukova, A. S. Shalygin, E. Y. Gerasimov, S. V. Tsybulya and O. N. Martyanov, *J. Sol. State Chem.*, **233**, 294 (2016).
32. R. Burch, S. E. Golunski and M. S. Spencer, *J. Chem. Soc. - Faraday Trans.*, **86**, 2683 (1990).
33. G. Wu, X. Wang, W. Wei and Y. Sun, *Appl. Catal. A Gen.*, **377**, 107 (2010).
34. Y. Liu, K. Sun, H. Ma, X. Xu and X. Wang, *Catal. Comm.*, **11**, 880 (2010).
35. P. Gao, F. Li, N. Zhao, F. Xiao, W. Wei, L. Zhong and Y. Sun, *Appl. Catal. A Gen.*, **468**, 442 (2013).
36. A. Le Valant, C. Comminges, C. Tisseraud, C. Canaff, L. Pinard and Y. Pouilloux, *J. Catal.*, **324**, 41 (2015).
37. C. Tisseraud, C. Comminges, T. Belin, H. Ahouari, A. Soualah, Y. Pouilloux and A. Le Valant, *J. Catal.*, **330**, 533 (2015).